

Specific heat and upper critical fields in KFe_2As_2 single crystals

M. Abdel-Hafiez,* S. Aswartham, S. Wurmehl, V. Grinenko,
S.-L. Drechsler, S. Johnston, A.U.B. Wolter-Giraud, and B. Büchner

Leibniz-Institute for Solid State and Materials Research, (IFW)-Dresden, D-01171 Dresden, Germany

H. Rosner

Max-Planck-Institute for Chemistry of Solid Materials (CPfS), Dresden, Germany

(Dated: March 15, 2012)

We report low-temperature specific heat measurements for high-quality single crystalline KFe_2As_2 ($T_c \approx 3.5$ K). The investigated zero-field specific heat data yields an unusually large nominal Sommerfeld coefficient $\gamma_n = 94(3)$ mJ/mol K² which is however affected by extrinsic contributions as evidenced by a sizable residual linear specific heat and various theoretical considerations including also an analysis of Kadowaki-Woods relations. Then KFe_2As_2 should be classified as a weak to intermediately strong coupling superconductor with a total electron-boson coupling constant $\lambda_{\text{tot}} \sim 1$ (including a calculated weak electron-phonon coupling constant of $\lambda_{\text{el-ph}} = 0.17$). From specific heat and ac susceptibility studies in external magnetic fields the magnetic phase diagram has been constructed. We confirm the high anisotropy of the upper critical fields $\mu_0 H_{c2}(T)$ ranging from a factor of 5 near T_c to a slightly reduced value approaching $T = 0$ for fields $B \parallel ab$ and $\parallel c$ and show that their ratio Γ slightly exceeds the mass anisotropy of 4.35 derived from our full-relativistic LDA-band structure calculations. Its slight reduction when approaching $T = 0$ is not a consequence of Pauli-limiting as in less perfect samples but point likely to a multiband effect. We also report irreversibility field data obtained from ac susceptibility measurements. The double-maximum in the T -dependence of its imaginary part for fields $B \parallel c$ indicates a peak-effect in the T -dependence of critical currents.

PACS numbers: 74.25.-q, 74.25.Bt, 74.25.Ha

I. INTRODUCTION

Since the discovery of superconductivity (SC) in an electron doped LaFeAsO (La-1111) compound with a superconducting transition temperature $T_c \sim 26$ K [1], iron pnictides are of great interest in fundamental condensed matter physics due to their large variety of structural, magnetic and electronic properties. In order to understand the nature of superconductivity in Fe pnictides a huge amount of theoretical and experimental studies has been performed but nevertheless many questions have not been answered yet, such as the symmetry of the order parameter and the pairing mechanism as well as their relation to the magnetic properties. In this situation, low- T specific heat and magnetic susceptibility measurements might be helpful since they provide insight into many-body physics via the renormalization of such physical quantities as: the Sommerfeld coefficient γ_{el} (a measure of the renormalized density of states), the irreversibility field H_{irr} , the upper critical field H_{c2} , its anisotropy etc. all are important factors which affect the superconducting and the normal state properties as well. In particular, they can shed light on the Fermi surface topology and other relevant aspects of the electronic structure. To address the role of magnetism in the formation of the superconducting state the heavily hole doped KFe_2As_2 is worth to be studied due to its

distinctive characteristics with respect to other stoichiometric 122 and 1111 Fe-pnictide compounds: (i) there is no static magnetic ordering in the sense of an ordinary spin-density wave (SDW) or an orthorhombic structural transition [2, 3]. (ii) Superconductivity occurs in relatively dirty samples near 2.8 K [4] and increases in cleaner high-quality single crystals up 3.5 to 3.7 K [3]. (iii) Remarkably, no nesting of the Fermi surface was detected in contrast to e.g. $\text{Ba}_{0.6}\text{K}_{0.4}\text{Fe}_2\text{As}_2$ [5, 6]. However, a neutron scattering study of heavily hole doped superconducting KFe_2As_2 revealed well-defined low-energy incommensurate spin fluctuations at $[\pi(1 \pm 2\delta), 0]$ with $\delta = 0.16$ [7]. This is different from the previously observed commensurate antiferromagnetism (AFM) of electron-doped AFe_2As_2 ($A = \text{Ba}, \text{Ca}, \text{or Sr}$) at low energies. Additionally, de Haas-van Alphen [8] and cyclotron resonance [9] studies of KFe_2As_2 revealed a strong mass enhancement of the quasi-particles. Furthermore, it exhibits a very large anisotropy as compared with less hole-doped members of the 122-family and other Fe-pnictide and chalcogenide superconductors [10] After naturally electronically more anisotropic 1111 and $\text{Tl}_{1-y}\text{Rb}_y\text{Fe}_{1-\delta}\text{Se}_2$ with $y \sim 0.4, \delta \sim 0.3$ superconductors showing only slightly larger or comparable slope anisotropies of ~ 5 to 6 K-122 belongs to the most anisotropic pnictides [11]. A complete understanding of their critical field slopes near T_c is still missing due to the complex interplay of pair-breaking impurities and the symmetry of the superconducting order parameter [12].

The magnetic phase diagram of KFe_2As_2 has been studied via resistivity measurements on single crystals

*Electronic address: m.mohamed@ifw-dresden.de

[4], however, its determination using thermodynamic bulk techniques on single crystalline material is lacking up to now [13, 14]. In the context of recently discovered very high surface upper critical field H_{c3} with $H_{c3}(T)/H_{c2}(T) \sim 4.4$ for the external field \parallel to the ab -plane in $\text{K}_{0.73}\text{Fe}_{1.68}\text{Se}_2$ [15] is noteworthy, because for that direction the nucleation starts already much higher at H_{c3} and resistivity and/or ac susceptibility measurements might in principle lead to a confusion between H_{c2} and H_{c3} suggesting this way an overestimated anisotropy of the upper critical fields. Hence, for this geometry, specific heat studies of high-quality single crystals are mandatory to address their bulk anisotropy.

Here we present low- T specific heat and ac magnetization studies on high-quality superconducting KFe_2As_2 single crystals with a larger T_c and a much higher residual resistivity ratio as compared to the first single crystals used for an upper critical field study for KFe_2As_2 by Terashima *et al.* [4], where a large anisotropy ratio of the upper critical fields as well as for the electric resistivity perpendicular and parallel to the ab -plane have been reported. The obtained data are analyzed within the framework of various theoretical approaches. In particular, we found good agreement with the electron mass anisotropy derived from density functional theory (DFT) considering in- and out-of plane plasma frequencies and Fermi velocities.

II. EXPERIMENTAL

Single crystals of KFe_2As_2 have been grown using a self-flux method with $\text{K}:\text{Fe}:\text{As}$ in the molar ratio of 1:4:4. All preparation steps like weighing, mixing, grinding and storage were carried out in an Ar-filled glove-box. As a first step the appropriate amounts of the precursor materials FeAs and Fe_2As were thoroughly grinded in an agate mortar, secondly the exact amount of weighed metallic K was deposited at the bottom of an alumina crucible, where on top of it the well grinded mixture is placed carefully, finally sealed in a niobium crucible. The sealed crucible assembly is placed in a vertical furnace, heated up to 1373 K and cooled down to 1023 K with a rate of 2 K/hour. Finally the furnace is cooled very fast from 1023 K to room temperature. All crystals are grown with layer-like morphology and they are quite easy to cleave along the ab plane. The quality of the grown single crystals was assessed by complementary techniques. Several samples were examined with a Scanning Electron Microscope (SEM Philips XL 30) equipped with an electron microprobe analyzer for a semi-quantitative elemental analysis using the energy dispersive x-ray (EDX) mode. The composition was estimated by averaging over several different points of the platelet-like single crystals and is found to be consistent and homogeneous with a 122 structure within the instrumental error bars. Typical crystal sizes with a rectangular shape were about $1.2 \times 0.5 \text{ mm}^2$ and a thickness of $50 \mu\text{m}$ along the c -axis. All crystals

exhibit very similar T_c -values (see the insets of Figs. 2 and 8) within the experimental error of about 0.25 K.

Low-temperature specific heat and ac magnetization have been determined using a Physical Property Measurement System (PPMS from Quantum Design). The specific heat data were measured using a relaxation technique. For the measurements at $H \parallel ab$ a small copper block has been used to mount the sample on the specific heat puck. The heat capacity of the copper block was determined in a separate measurement and its value has been subtracted from the raw data of KFe_2As_2 .

III. RESULTS AND DISCUSSIONS

A. ac magnetization measurements

Figure 1 depicts the T -dependence of the volume ac susceptibilities (χ'_v and χ''_v) of our KFe_2As_2 single crystal. The measurements were done in an ac field with an amplitude $B_{ac} = 5 \text{ Oe}$, a frequency $f = 1 \text{ kHz}$ and DC fields up to 5 T parallel to the ab -plane as shown in Fig. 1a and parallel to the c axis in Fig. 1b. Special care has been taken to correct the magnetization data for demagnetization effects, where the demagnetization factor has been estimated based on the crystal dimensions [16]. The ac susceptibility measurements can be used for an investigation of the flux dynamics in superconductors [17–19]. The imaginary part χ''_v is related with the energy dissipation in a sample and the real part χ'_v is related with the amount of screening. Both these functions depend on the ratio between skin depth δ_s and the sample dimension L in the direction of the flux penetration. In the normal state $\delta_s \sim (\rho_n/f)^{0.5}$, where ρ_n is the normal state resistivity and f is the frequency. In the superconducting state the skin depth $\delta_s \propto \lambda_L$ if an external magnetic field is below the first critical field H_{c1} , where λ_L is the London penetration depth. For magnetic fields above H_{c1} , $\delta_s \propto L_B$, where $L_B \sim B_{ac}/J_c$ is the Bean's penetration depth and J_c is the critical current density. In general, if $L \ll \delta_s$ an ac field completely penetrates the sample and thus the susceptibility is small. In the case, if $L \gg \delta_s$, most of the sample volume is screened, therefore, $4\pi\chi'_v = -1$ and $\chi''_v \rightarrow 0$. In accordance with this the ac susceptibility data measured at low T confirm the bulk superconductivity of our KFe_2As_2 single crystal (Fig. 1). $T_c \sim 3.6(1) \text{ K}$ has been extracted from the bifurcation point between χ'_v and χ''_v susceptibilities as shown in the inset of Fig. 1b. This point is related with a change in the linear resistivity due to the superconducting transition. It can be also used for the determination of the T -dependence of the upper critical field H_{c2} from ac susceptibility data measured at various DC fields [17].

At $T < T_c$ the function χ''_v increases with decreasing temperature and some value of $T = T_{irr}$ where ($L \sim \delta_s$) χ''_v has a maximum (see Fig. 1). The above discussed Bean's approximation predicts that the T -dependence of the peak in χ''_v follows the T -dependence of the critical

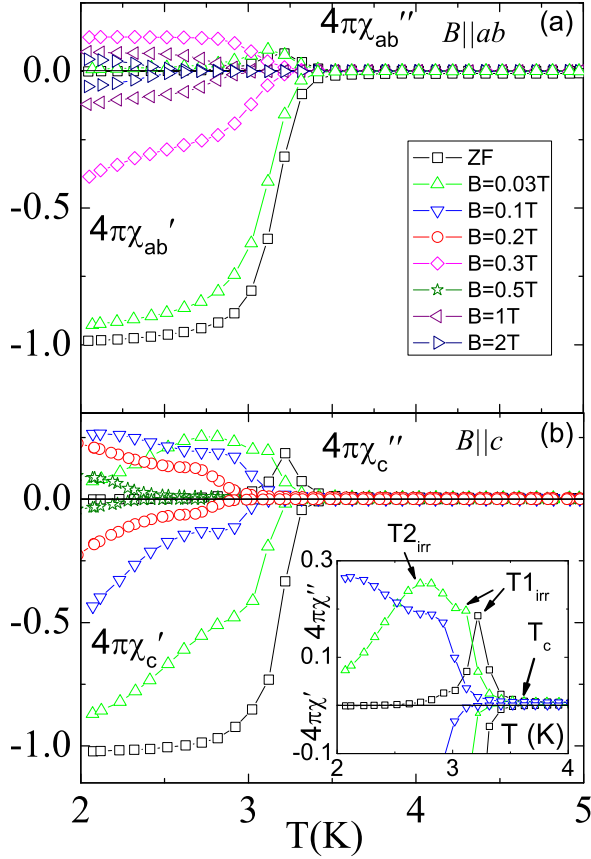


FIG. 1: (Color online) (a) The T -dependence of the complex ac susceptibility components $4\pi\chi'_v$ and $4\pi\chi''_v$ of KFe_2As_2 has been measured in an ac field with an amplitude 5 Oe and a frequency of 1 kHz upon warming in different DC magnetic fields after cooling in zero magnetic field with (a) $B \parallel ab$ and (b) $B \parallel c$. The sharp superconducting transition with $\sim 100\%$ superconducting volume fraction indicates the bulk nature of superconductivity and the high quality of our crystal. The inset shows the criteria used to obtain T_c and T_{irr} ; for details see text.

current density J_c . Thus, one might relate T_{irr} with an irreversibility temperature and use its DC field dependence to obtain the irreversibility field H_{irr} [19]. However, we remind the reader that H_{irr} defined this way is not the 'true' irreversibility field since by definition H_{irr} is the field at which $J_c = 0$. From this point of view it is better to use dc magnetization data to obtain the irreversibility line. In general, we observed a rough agreement between H_{irr} obtained from dc and ac susceptibility data but the large value and the strong T -dependence of the normal state dc susceptibility lead to a large uncertainty in determination of the H_{irr} . Therefore, to obtain the irreversibility line we used ac susceptibility data. (The DC susceptibility data will be presented elsewhere [20]). Thus, with some cautions we relate the maximum in the T -dependence of χ''_v to T_{irr} . It can be seen in Fig. 1b that at non-zero $B_{DC} \parallel c$ the single maximum in

χ''_v splits into two features at $T1_{irr}$ and $T2_{irr}$. Therefore, for $B_{DC} \parallel c$ we defined two different 'irreversibility' fields $H1_{irr}$ and $H2_{irr}$. The T -dependence of these fields is plotted in Fig. 6.

B. Specific heat studies

Figure 2 shows the T -dependence of the zero-field specific heat measured down to 0.4 K. A clear sharp anomaly was observed near 3.5 K in agreement with the magnetization data. In order to determine the zero-field normal state Sommerfeld coefficient γ_n , the specific heat can be plotted for $T > T_c$ as c_p/T versus T^2 following

$$c_p = \gamma_n T + \beta_3 T^3 + \beta_5 T^5 + \dots, \quad (1)$$

with γ_n and β_3 , β_5 as the nominal electronic and lattice coefficients, respectively. The obtained values for our KFe_2As_2 sample are $\gamma_n = 94(3)$ mJ/mol K² and $\beta_3 = 0.79$ mJ/mol K⁴ and $\beta_5 = 6.09 \cdot 10^{-4}$ mJ/mol K⁶. Our γ_n value compares very well with $\gamma_n = 93$ mJ/mol K² reported in Ref. [21]. From the relation for the Debye temperature, $\theta_D = (12\pi^4 R Z / 5\beta_3)^{1/3}$, where R is the molar gas constant and $Z = 5$ is the number of atoms per formula unit, we obtain $\theta_D = 214$ K.

Notice the enhanced value of γ_n for KFe_2As_2 as compared to other stoichiometric and nonstoichiometric 122 compounds or to any other superconducting iron pnictide or chalcogenide to the best of our knowledge. The low values of γ_n for BaFe_2As_2 and SrFe_2As_2 are not surprising since large parts of its Fermi surface are gapped due to the well-known magnetic spin density wave (SDW) transition at high temperatures. Hence, in these cases a comparison with a hole doped system where the SDW transitions are suppressed is more meaningful. For instance, for the closely related, nearly optimal hole-doped systems $\text{Ba}_{0.68}\text{K}_{0.32}\text{Fe}_2\text{As}_2$ ($T_c = 38.5$ K) [22], $\text{Ba}_{0.6}\text{K}_{0.4}\text{Fe}_2\text{As}_2$

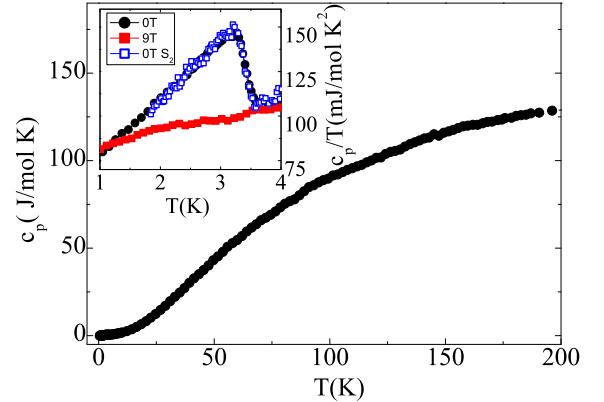


FIG. 2: (Color online) The T -dependence of the zero-field specific heat of KFe_2As_2 for $400 \text{ mK} \leq T \leq 200 \text{ K}$. The inset shows c_p/T versus T of our 0 T and 9 T data together with the zero-field of another sample (S₂) shows the same $T_c(H)$ behavior down to 1.8 K.

($T_c = 36.5$ K) [23] or $\text{Ba}_{0.65}\text{K}_{0.35}\text{Fe}_2\text{As}_2$ ($T_c = 29.4$ K) [24], the Sommerfeld parameters $\gamma_n = 50.0$, 63.3 and 57.5 $\text{mJ mol}^{-1}\text{K}^{-2}$, respectively, have been reported. In view of their much higher T_c -values, ascribed by the authors to an essential contribution from strong coupling corrections with $\lambda \sim 2$ [22] for the electron-boson coupling constant (spin fluctuation mediated interband coupling) and a comparable bare value of $\gamma_b \sim 10 \text{ mol}^{-1}\text{K}^{-2}$ (see below) according to DFT-band structure calculations the unusual large value for KFe_2As_2 reported above provides a surprising puzzle. However, it can be somewhat reduced, if there is an essential *extrinsic* contribution to the system of itinerant charge carriers, e.g. due to defect states with low-energy excitations [20]. To be consistent with that analysis we are forced to assume, that KFe_2As_2 is *not* in the strong coupling limit which seems to be natural in view of its low T_c -value (to be discussed within the framework of Eliashberg-theory elsewhere). The general situation, independent on the

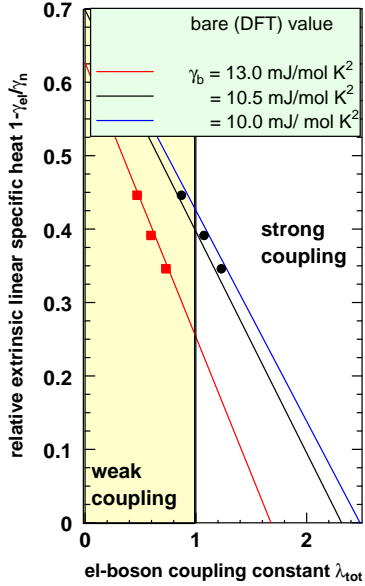


FIG. 3: (Color online) The relative extrinsic linear specific heat coefficient of KFe_2As_2 using the experimentally observed nominal $\gamma_n = 94 \text{ mJ/mol} \cdot \text{K}^2$ vs. the total electron-boson coupling constant λ_{tot} given by Eqs. (4,7) for various bare γ_b -values obtained from density of states as calculated by various DFT codes [22,25,26] (see text) and using a typical high-energy renormalization factor of $\eta = 2.7$ (see Eq. (4)). The data points show the results of simulations within single band *d*-wave Eliashberg theory to reproduce $T_c = 3.5$ K and a spectral density for spin fluctuations adopted from recent INS data [7] and including also a weak electron-phonon interaction and a weak Coulomb pseudopotential μ^* (details will be discussed elsewhere).

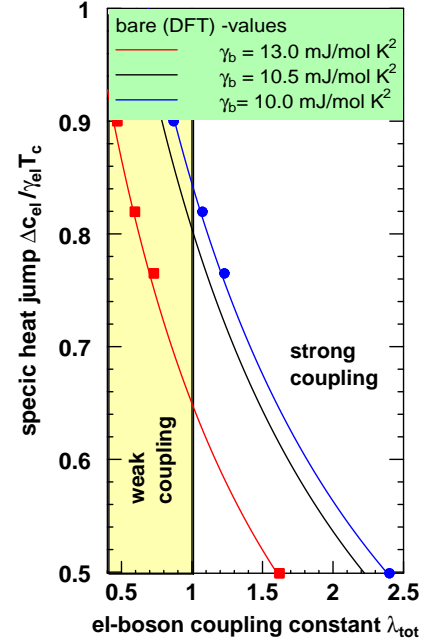


FIG. 4: (Color online) The normalized specific heat jump at T_c vs. the phenomenological total electron-boson coupling constant λ and various DFT-derived bare linear specific heat values [22,25,26] Red and blue symbols: results using the corresponding γ_{el} values from Fig. 3 extended by two strong coupling points for $\gamma_{el} = \gamma_n$ and the experimental value of $\Delta c_{el}/T_c = 45.6 \text{ mJ/ mole} \cdot \text{K}^3$)

strength of the electron-boson coupling regime and the symmetry of the order parameter, is plotted in Figs. 3 and 4 using the calculated DFT-values γ_b [22, 25, 26] as convenient bare values. Thereby the high-energy renormalization $\eta = 2.7$ as derived from the calculated DFT plasma frequencies of 2.58 eV [25] and 2.56 eV [26, 27] and the expected experimental unscreened plasma frequency of about 1.55 eV have been taken into account [28]. There are at least two experimental hints which clearly point to the existence of such an extrinsic subsystem which manifest itself in a substantial residual linear specific heat visible at very low- T at ambient fields (see Fig. 8) and in high fields of about 9 T where the superconductivity is well suppressed (see inset of Fig. 2). From the latter one estimates $\gamma_{el} \leq 70 \text{ mJ/mol K}^2$. In the next section we will provide theoretical arguments in favor of a significantly reduced intrinsic Sommerfeld term γ_{el} .

C. Theoretical estimates of the thermal mass enhancement

1. Kadowaki-Woods analysis

The weak coupling result can be understood at a qualitative level also by analyzing the so called Kadowaki-Woods relation (KWR) $\kappa_{\text{KWR}} = A_\rho/\gamma_v^2$, where A_ρ describes the T^2 -contribution to the resistivity at very low T : $\rho(T) = \rho_0 + A_\rho T^2$ observed so far only in few very clean samples [25] with extremely large residual resistivity ratio $\rho(300\text{K})/\rho(5\text{K}) \approx 500$ and γ_v is the volumetric Sommerfeld coefficient. The latter is related to the usually used molar quantity γ_0 in the present case with two KFe_2As_2 units per unit cell by the relation

$$\gamma_v = 2\gamma_0/N_A V_u$$

where N_A denotes the Avogadro's number and $V_u = 204.2\text{\AA}^3$ is the unit cell volume of KFe_2As_2 . Then following Hussey [29], one has for the case of a (quasi)-2D system with cylindrical Fermi surface sheets

$$\kappa_{\text{KWH}} = \frac{A_\rho}{\gamma_v^2} = \frac{72\pi\hbar}{e^2 k_B^2} \frac{ac^3}{k_{\text{F,el}}^3} = \propto n^{-1.5}. \quad (2)$$

Notice the cancellation of many-body renormalizations on the r.h.s. and the different exponent -1.5 for the density n as compared with $\propto n^{-2}$ within a similar expression proposed recently and given here for comparison also for the 2D-case, only: [30]:

$$\kappa_{\text{KWJ}} = \frac{A_\rho}{\gamma_{0,\text{el}}^2} = \frac{81\pi\hbar}{4k_B^2 e^2 n^2} \propto n^{-2}. \quad (3)$$

Since in the stoichiometric case of K-122 there is exactly one hole in the three bands (i.e. per formulae unit) which cross the Fermi energy one obtains for the corresponding electron density $n_{\text{el}} = 4.94 \times 10^{28} \text{m}^{-3}$ and

$$k_{\text{F,el}} = \sqrt{2\pi n c} = 2.07 \cdot 10^{-10} \text{m}^{-1}$$

for the 2D-effective Fermi wave vector of electrons. Inserting our value of $k_{\text{F,el}}$ into Eq. (2), one arrives at $\gamma_v = 0.67 \text{ mJ/K}^2 \text{cm}^3$ or $\gamma_{0,\text{el}} \approx 41.05 \text{ mJ/K}^2 \text{mol} < \gamma_n$. Using instead Eq. (3) one obtains a slightly smaller value $\gamma_{0,\text{el}} \approx 36.95 \text{ mJ/K}^2 \text{mol}$ which however again is significantly smaller than our nominal value $\gamma_n \approx 94 \text{ mJ/K}^2 \text{mol}$. Thereby in both cases of Eqs. (2,3) the experimental value $A_\rho = 3 \times 10^{-2} \mu\Omega \text{cm}$ has been used as reported in Ref. 25. Thus, our empirical value of about $60 \text{ mJ/K}^2 \text{mol}$ [20] can be regarded as reasonable number. In view of the idealized electronic structure in terms of cylindric FSS adopted above, a more realistic and sophisticated multiband analysis is desirable. To illustrate this point we consider the simple case when all four FSS would give the same contribution to the resistivity and to the specific heat. Applying the Kadowaki-Woods relation first to such a hypothetical single FSS we would arrive

finally at $73.9 \text{ mJ/K}^2 \text{mol}$ in case of Eq. (3). Since different individual residual resistivities ρ_i $i = 1-4$ lower these values, we regard these two numbers as upper and lower bounds for a more realistic $\gamma_{0,\text{el}}$ somewhere in between. More theoretical microscopic studies including also the determination of the individual residual resistivities are necessary to improve the accuracy of these Kadowaki-Woods type relations for pronounced multiband systems. Note that our empirical value of about 60 is very close to the mean value $0.5(36.95+73.9) = 55.45$ and 78.57 in case of Eq. (2). A more detailed consideration will be given elsewhere. Anyhow, considering also available data for the in-plane penetration depth (or the condensate density) in the superconducting state at very low T , one arrives at similar estimates (see below) and we strongly believe that the nominal value of about $94 \text{ mJ/K}^2 \text{mol}$ given above and similar numbers found in the recent literature [21] as well, do significantly *overestimate* the contribution from the itinerant electrons which bear the superconductivity.

The nominal value γ_n should be compared with the calculated quantity of $\gamma_b = 10.2$ to 13.0 mJ/mol K^2 from DFT (density functional theory) based band structure calculations [25, 26] regarded as the unrenormalized bare quantity. The renormalization happens in two steps at different energy scales: a first one at high-energies is governed by the Coulomb interaction and/or Hund's rule coupling and a second one at low-energies governed by the interaction of the quasi-particles with various bosonic excitations (phonons, paramagnons, magnons etc.). The high-energy renormalization yields for typical transition metals a mass enhancement by a factor two to three as evidenced by a general band squeezing as observed for instance in ARPES measurements [5, 6] or in optical measurements comparing calculated and measured unscreened plasma frequencies. In fact, taking a typical 122 experimental in-plane plasma frequency of 1.55 eV [28] to be compared with the calculated DFT value of 2.56 eV to 2.58 eV [25, 26] mentioned above. Then, this high-energy mass enhancement can be estimated by a large factor of $\eta \approx 2.7$ in accord with the high-energy band "squeezing" factor of about 2 to 3 as seen by ARPES [5, 6]. Thus, one is left with an effective quasi-particle (qp) γ_{qp} quantity of about 30 to 40 mJ/mol K^2 to be compared with our empirical estimate of about 60 mJ/mol K^2 :

$$\begin{aligned} \gamma_{\text{el}} &= \gamma_{\text{qp}}[1 + \lambda_{\text{ph}} + \lambda_{\text{sf}}], \\ \gamma_{\text{qp}} &= \eta\gamma_b, \\ \eta &\approx \Omega_{\text{pl,DFT}}^2/\Omega_{\text{pl,opt}}^2, \end{aligned} \quad (4)$$

where λ_{ph} is the electron-phonon coupling constant, λ_{sf} is the enhancement due to spin fluctuations (antiferromagnetic paramagnons), and $\eta > 1$ denotes the high-energy renormalization. In case of Fe-based superconductors the conventional electron-phonon interaction is weak yielding $\lambda_{\text{ph}} \leq 0.2$ [31] which is insufficient to explain the large γ_{el} -value obtained from specific heat measurements. A similar value has been found also for KFe_2As_2 : $\lambda_{\text{ph}} \approx 0.17$

(details of this DFT based calculation will be given elsewhere). Taking this into account, we may finally estimate that $\lambda_{sf} \lesssim 1$ in the case of KFe_2As_2 .

2. Penetration depth and condensate density

The conclusion about weak electron-boson coupling is also supported using the experimental value of the in-plane penetration depth extrapolated to $T = 0$: $\lambda_{ab,L} \approx 203$ nm (measured at 50 mK) [32]. Following Refs. 27, 33, 34 one has from the *renormalized* plasma frequency which enters the penetration depth rewritten in convenient units

$$\Omega_{pl}[\text{eV}]\lambda_L[\text{nm}] = 197.3\sqrt{DNZ_m}, \quad DNZ_m > 1, \quad (5)$$

where $N = n_{\text{tot}}/n_s$ is the reciprocal number of the conduction electron density involved in the superconducting condensate, $Z_m \approx (1 + \lambda_{\text{tot}}(0))$ describes the dynamical mass renormalization and $D = (1 + \delta)(1 + f)$ with $\delta, f > 1$ describes the effect of disorder and fluctuations of competing phases. In the clean limit one has $\delta \rightarrow 0$. For the sake of simplicity we will ignore the influence of fluctuations. Using $\hbar\Omega_{pl} = 1.55$ eV for the expected unscreened experimental plasma frequency, (i.e. the experimental high- T plasma frequency with no or small renormalizations due to the electron-boson couplings) one has

$$2.64 \frac{n_s}{n_{\text{tot}}} = (1 + \lambda_{ph} + \lambda_{sf})(1 + \delta), \quad (6)$$

where $\delta \sim 1/3$ measures the disorder and the reciprocal gap amplitude related parameter close to that in the clean limit (i.e. $\delta \ll 1$). Furthermore for the sake of simplicity we will assume that all electrons are involved in the superconducting condensate, i.e. $N \equiv 1$ (just for illustration see also the special case $n_s/n \approx 0.74$ mentioned in our remark [35]). Then, one arrives at the constraint [36]:

$$\lambda_{\text{tot}} = \lambda_{ph} + \lambda_{sf} \approx 0.97, \quad \text{or } \lambda_{sf} \approx 0.8. \quad (7)$$

in accord with a close estimate from $\gamma_{el} \sim 60$ mJ/K² mol and $\gamma_b \approx 10.5$ mJ/K²mol from DFT calculations for the bare density of states [26].

D. The upper critical fields $H_{c2}(T)$ and their anisotropy

Figs. 5-7 summarize the T -dependence of the specific heat data c_p of the investigated KFe_2As_2 single crystal for various magnetic fields applied parallel and perpendicular to the ab -plane. With increasing applied magnetic field in both directions, the superconducting anomaly shifts and broadens systematically to lower T and is also

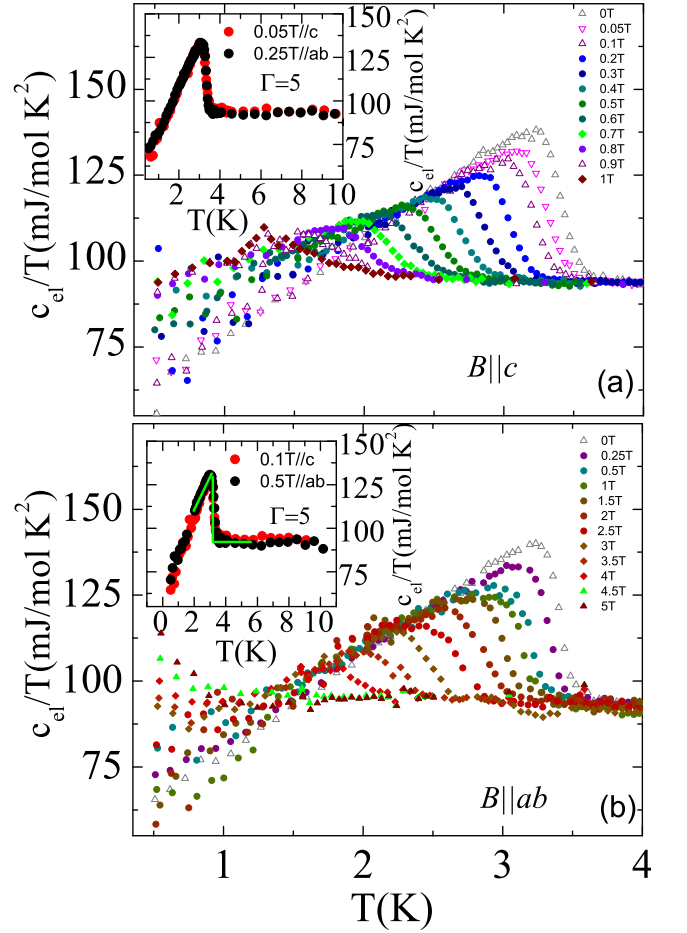


FIG. 5: (Color) The electronic specific heat coefficient c_{el}/T of KFe_2As_2 (after subtracting the phonon contribution) for both directions $B \parallel c$ and $B \parallel ab$ as shown in (a) and (b), respectively. In order to determine the T_c of KFe_2As_2 , an entropy - conserving construction has been used as shown with a green line in the inset of (b). The insets of the upper and lower panel show two data sets with the same T_c value for the two directions confirming our anisotropy ratio $\Gamma \sim 5$.

reduced in height. In an applied magnetic field of 9 T, superconductivity is completely suppressed for both directions of our crystal. In order to analyze the phase diagram of the field dependence of T_c , we used an entropy-conserving construction of the electronic specific heat to determine T_c of both orientations as shown in Fig. 5. Then, in a very first step the upper critical field and its slope near T_c can be estimated by the Ginzburg Landau (GL) equation [37, 38] (strictly speaking valid near T_c , only):

$$H_{c2} = H_{c2}(0) \left[\frac{1 - t^2}{1 + t^2} \right], \quad (8)$$

where $t = T/T_c$. The upper critical field values at $T = 0$ have been evaluated to $\mu_0 H_{c2}^{(c)}(0) = 1.8$ T and $\mu_0 H_{c2}^{(ab)}(0) = 8.6$ T and the fits are shown via dashed black lines in Fig. 6. In the case of H_{c2} obtained from ac susceptibil-

ity data (see above Fig. 1) we derive at slightly different values of $\mu_0 H_{c2}^{(c)}(0) \approx 1.9$ T and $\mu_0 H_{c2}^{(ab)}(0) \approx 7.5$ T, respectively (dashed red curves).

It is interesting to compare the obtained and extrapolated to $T = 0$ anisotropy ratio for the upper critical field of 4 to 5 with that ratio for the penetration depth [39] (i.e. $\lambda_{L,ab} = 194,3$ nm and $\lambda_{L,c} = 510.3$ nm taken at $T = 20$ mK) which yields 2.63, only. In fact, for a simple one-band or separable multiband models [12] including a phenomenological mass anisotropy, one would expect

$$\Gamma_0 \approx \left(\frac{m_c}{m_{ab}} \right)^{1/2} = \frac{\lambda_{L,c}(0)}{\lambda_{L,ab}(0)} = \frac{H_{c2\parallel ab}(0)}{H_{c2\parallel c}(0)}. \quad (9)$$

From full relativistic DFT-calculations an out of plane plasma frequency of 0.61 eV has been obtained [26] which suggests an mass anisotropy of 4.38 slightly exceeding the value of 3.27 for Ba-122 [40] Thus, the observed

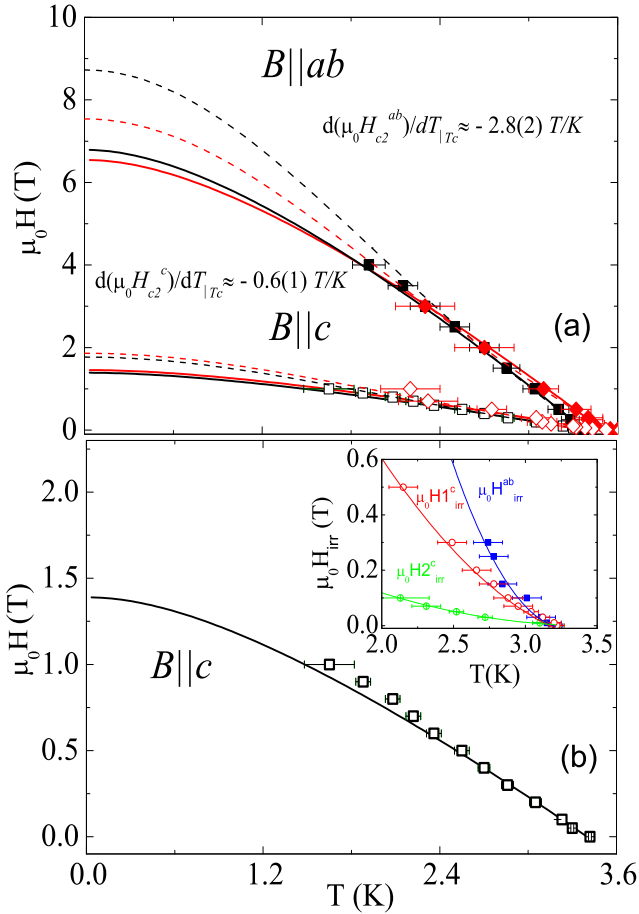


FIG. 6: (Color online) Phase diagram of $\mu_0 H_{c2}(T)$ for KFe₂As₂ with the magnetic field applied parallel and perpendicular to the c axis from specific heat (black symbols) and ac susceptibility measurements (red symbols). Solid lines: theoretical curves based on the WHH model ($\alpha = 0$ and $\lambda_{so} = 0.1$). Dashed curves: GL theory. Inset: T -dependence of H_{irr} obtained from ac susceptibility measurements as discussed in the text.

anisotropy derived from the upper critical fields exceeds this value whereas the penetration depth gives a slightly smaller value. We ascribe this small deviation of our empirical Γ from the simple mass anisotropy to

(i) the anisotropy of the pairing interaction and consequently also of the order parameter and/or oppositely of the depairing interaction. In Ref. 39 which might additionally enhance $H_{c2\parallel ab}$ and suppress $\lambda_{L,ab}$ or vice versa the corresponding c -components. For instances, the anisotropic screening and significantly anisotropic plasma frequencies might cause an anisotropic Coulomb pseudopotential μ^* . The in-plane anisotropy observed for ordered magnetic structures should in case of a magnetic spin fluctuation bases mechanism act in a similar way.

(ii) Furthermore, one should take into account, that strictly speaking, the upper critical fields and the penetration depth at $T = 0$ probe various subgroups of electrons with different Fermi-velocity dependent weights: whereas the penetration depth probes more sensitively fast electrons $\lambda_{L,i}^{-2} \propto \Omega_{pl,i}^2$, where $\Omega_{pl,i}$ denotes the corresponding i^{th} subgroup plasma frequency and the total penetration depth is given by $\lambda_L^{-2} = \sum_i \lambda_{L,i}^{-2}$. In contrast, the upper critical fields are more sensitive to slow electrons since $H_{c2\parallel ab} \propto (\Phi_0/v_x v_z)$, where Φ_0 denotes the flux quantum. Finally,

(iii) anisotropic impurity scattering rates might also affect Γ_0 .

Another possibility to estimate roughly the upper critical field $H_{c2}(0)$ is to consider the single-band Werthamer-Helfand-Hohenberg (WHH) formula [41] with the Maki parameter $\alpha = 0$ and $\lambda_{so} = 0.1$ which is a reasonable value of spin orbital scattering for Fe-based superconductors [42]. As shown with solid lines in Fig. 6, the specific heat and ac magnetization H_{c2} data for $B \parallel ab$ are perfectly described by the WHH model with an average slope $-d(\mu_0 H_{c2}^{ab})/dT \approx 2.8(2)$ T/K while for $H \parallel c$ the single-band WHH model with $-d(\mu_0 H_{c2}^{(c)})/dT = 0.55(5)$ T/K underestimates the experimental data obtained from the specific heat measurements (see lower panel of Fig. 6). This deviation is particularly visible in the case of H_{c2} obtained from the ac magnetization data where we used $-d(\mu_0 H_{c2}^{(c)})/dT = 0.6(1)$ T/K. From these values the upper critical fields $\mu_0 H_{c2}(0)$ are found to be ~ 1.4 T and ~ 7 T for the c and ab direction, respectively. The observed small difference between H_{c2} obtained from the specific heat and the ac magnetization data is expected since these methods naturally implies different criteria for T_c determination.

In general, in case of multi-band superconductivity the low- T H_{c2} -curve may exceed the single-band WHH predictions [43]. Therefore, we suppose that the observed deviation from the single band WHH model is related to multi-band effects. Additionally, indication for a two-band like behavior of our single crystal was observed in zero field specific heat measurements (see below). Anyhow, using typical renormalized Fermi velocities $v_F \sim 4 \times 10^4$ m/s derived from preliminary ARPES-

data [6] and $T_c = 3.5$ K, one estimates also, in principle, within a two-band approach adopting s -symmetry [44, 45], a slope-value

$$H'_{c2,c} = -\frac{24\pi k_B^2 T_c \Phi_0}{7\zeta(3)\hbar^2 (c_1 v_1^2 + c_2 v_2^2)} \quad , \quad (10)$$

where $c_1 \rightarrow c_2 \rightarrow 1/2$ and $v_F \sim \sqrt{2}v_1, \sqrt{2}v_2$ in the case of a dominant interband pairing and $\zeta(3) \approx 1.202$, resulting in $-dH_{c2}^c/dT=0.69$ T/K near T_c which is already very close to our experimentally determined value and is also in accord with the renormalized Fermi velocity of $4 \cdot 10^6$ cm/s using the total bare velocity $1.77 \cdot 10^7$ cm/s from the full relativistic (not spin polarized) LDA calculations and the FSS averaged renormalizations contained in the intrinsic γ_{el} -value of about 60 mJ/K²mol estimated above. In comparison, the reported values determined via detailed resistivity studies on KFe₂As₂ single crystals yield lower values, i.e., $H_{c2}^c = 1.25$ T and $H_{c2}^{ab} = 4.47$ T, where a low value of $T_c = 2.8$ K, has been reported [4]. The anisotropy of the slopes near T_c *as measured* of about 5.35 is very close to the value found here: 5.09. The reported larger value of 6.8 seems to be a consequence of the extremely high anisotropic spin-orbit coupling $\lambda_{s0} = 0.36$ for $B \parallel ab$ and ∞ for $B \parallel c$ adopted in Ref. 4 in analyzing their data[46]. The reported *larger* absolute slope values might be interpreted as a hint for an impurity driven transition to an s -wave superconductor with $\langle \Delta \rangle_{FS} \neq 0$ with pair-breaking (see Eq. (A3) in Ref. 12). From our studies, further information about the anisotropy of KFe₂As₂ single crystals can be obtained, which is $\Gamma = H_{c2}^{ab}/H_{c2}^c \sim 5$ (see also the insets of Fig. 5). Surprisingly, this anisotropy value is comparable with Γ -values of e.g. NdFeAsO_{0.82}F_{0.18} [47] and LaFePO [48] showing a more anisotropic electronic structure (LaFeAsO: 9.2 to 10.8 and LaFePO: 4.16 to 5.04 and might be therefore ascribed to opposite anisotropies of the order parameter. On the other hand, it is considerably larger than a typical value of $\Gamma \sim 2$ and 2.6 found for nearly optimally hole doped BaKFe₂As₂ [49, 50], but lower than the ones determined for SmFeAsO_{0.85}F_{0.15} and La(O,F)FeAs thin films [10, 51].

The T -dependence of the irreversibility field H_{irr} obtained from χ''_v are shown in the inset of Fig. 6 (see above). The low value of H_{irr}^{ab} for $B \parallel ab$ is related with a large anisotropy and a weak pinning as expected in the case of clean single crystals. We attribute the $H1_{irr}^c$ with a peak effect in the T -dependence of the critical current J_c for $H \parallel c$ in accord with similar observations on YBCO single crystals [18] which exhibit a rather similar anisotropy of the upper critical field and therefore also a similar pinning behavior can be expected.

E. Aspects of the electronic specific heat in the superconducting state: the residual linear specific heat and the jump at T_c

The jump height of $\Delta_{c_{el}}/T_c \approx 45.6$ mJ/mol K² at T_c is found from our zero-field electronic specific heat data. This value exceeds the value which has been reported for a polycrystalline KFe₂As₂ sample [2] but by a factor of 2 lower than the one obtained for the nearly optimally-hole doped Ba_{0.6}K_{0.4}Fe₂As₂ [49]. For our estimated $\gamma_{el} \sim 60$ mJ/mol·K² the ratio $\Delta_{c_{el}}/\gamma_{el}T_c$ found to be enhanced as compared with the use of the nominal value: near about 0.76 vs. 0.49 (see Fig. 4), but it is still significantly lower than the result of the BCS weak coupling approximation: $\Delta_{c_{el}}/\gamma_{el}T_c=1.43$ [52], which points towards a multiple band (gap) with s, p - or d -wave nature of superconductivity. In particular, it is close to the value reported for the p -wave superconductor SrRuO₄ which exhibits 0.73 [53].

In a clean situation with negligible pair breaking ef-

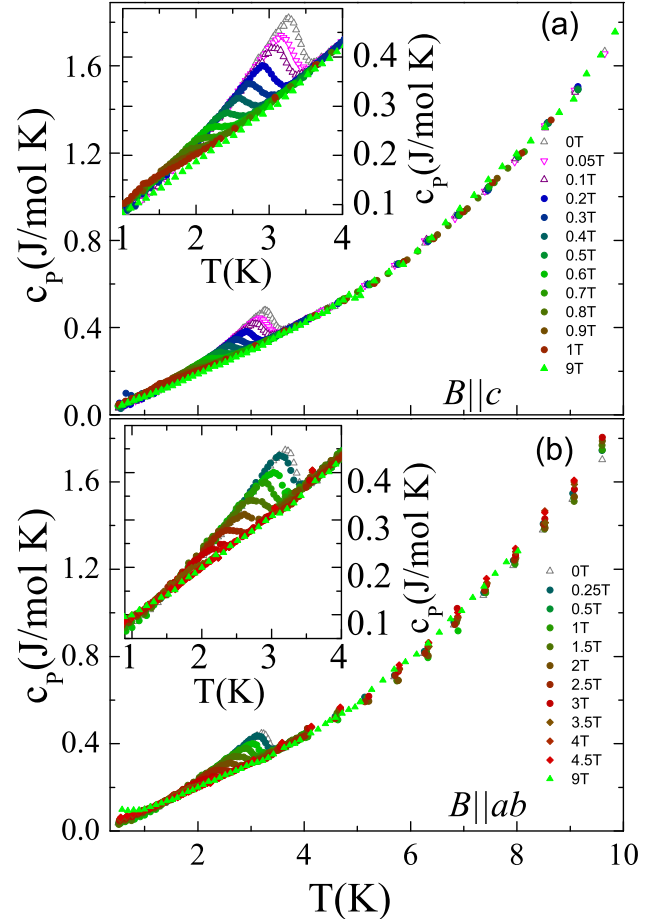


FIG. 7: (Color online) The T -dependence of the specific heat of KFe₂As₂ in various applied magnetic fields up to 9 T parallel to the c axis (a) and parallel to the ab plane (b). The insets of the upper and lower panel show a zoom into the superconducting state for both directions.

fects, the reduced jump of the specific heat $\Delta c_{el}/T_c \gamma_{el}$ as compared with that of a single s -wave superconductor might be related to unconventional superconductivity with nodes as discussed above and/or to pronounced multiband character with rather different partial densities of states and gaps. Furthermore, in relative dirty systems the unconventional superconductivity might be driven into an s -wave state. To illustrate the multiband character we adopt here for the sake of simplicity a simple effective weak coupling s -wave model like in Ref. 24. Another interesting issue we would like to address is what happened with the "extrinsic" linear specific heat at very low T . Thus, fitting the electronic part of the specific heat within a two-band model (see the blue curves in Fig. 8) admitting also a "residual" linear Sommerfeld part, we arrive at a relative large value of $\gamma_{res}(T \rightarrow 0) \approx 15 \text{ mJ/K}^2 \text{ mol}$ which might be related to (i) an "extrinsic" pair breaking contribution somewhat suppressed deep in the superconducting state [35]. Anyhow, we admit that the adopted s -wave analysis might provide only an upper limit, since for an unconventional pairing symmetry the spectral weight at low- T is enhanced. Furthermore the final density of states introduced by pair-breaking induced subgap states might also contribute to such a value. Thus, more sophisticated multiband models including interacting pair-breaking impurity states are necessary to settle this highly interesting problem. Due to its complexity it is however far beyond the present paper. Specific heat measurement below 0.2 K might be helpful to refine the value of γ_{res} . In this context the observation of substantial residual terms in other pnictide or chalcogenide superconductors is noteworthy. For instance in the systems $\text{FeTe}_{0.57}\text{Se}_{0.45}$ and Co-doped Ba-122 also a relatively large (8% and 25%, respectively) residual linear contribution have been observed [54, 55].

Finally, for completeness we list the gap values obtained in the present simple model for analyzing the T -dependence of our zero-field specific heat measurements down to 400 mK. The normalized zero-field electronic specific heat $c_{el}/\gamma_n T$ is shown in Fig. 8. First, we compare our data to the single-gap BCS theory (i.e. the weak coupling approach using $\Delta_0/k_B T_c = 1.76$ at T_c) and find that a single BCS-gap cannot be reconciled with our experimental data. From the plot in Fig. 8 it is evident that the specific heat jump is much lower than the BCS weak-coupling value for an s -wave superconductor. Below T_c , systematic deviations of the theoretical curve from the experimental data have been observed at both low- T and around T_c . This clearly indicates that $c_{el}/\gamma_{el} T$ of KFe_2As_2 cannot be described by the weak coupling BCS (single-)gap.

Since a single-gap scenario cannot describe our data, we applied a phenomenological two-gap model in line with multi-gap superconductivity in many compounds of the FeAs family reported by various experimental and theoretical studies on different compounds within this family [2, 56–58]. We have analyzed our data utilizing the

generalized α -model which has been proposed to account for the thermodynamic properties in multi-band, multi-gap superconductors like e.g. MgB_2 [59]. We remind the reader that in this approach the one-band expression:

$$\frac{S}{\gamma_{el} T_c} = -\frac{6\Delta_0}{\pi^2 k_B T_c} \int_0^\infty [f \ln f + (1-f) \ln(1-f)] dy, \quad (11)$$

$$\frac{c_{el}}{\gamma_{el} T_c} = t \frac{d(\frac{c_{el}}{\gamma_{el} T_c})}{dt}, \quad (12)$$

is straightforwardly generalized to the two-band case and entropy conservation is adopted for each band. In Eq. (11) the Fermi-function is denoted by $f = [\exp(\beta E + 1)]^{-1}$, $\beta = (k_B T)^{-1}$ and the energy of the quasiparticles is given by $E = [\epsilon^2 + \Delta^2(t)]^{0.5}$ with ϵ being the energy of the normal electrons relative to the Fermi surface. The integration variable is $y = \epsilon/\Delta_0$. (S) and (C) is the thermodynamic properties and $t = T/T_c$ is the reduced temperature. In Eq. (11) the scaled gap $\alpha = \Delta_0/k_B T$ is the only adjustable fitting parameter. The temperature dependence of the gap is determined by $\Delta(t) = \Delta_0 \delta(t)$, where $\delta(t)$ is approximately described by the data taken from the table in Ref. [60]. In case of two gaps the thermodynamic properties are obtained as the sum of the contributions from the two gaps, i.e., $\alpha_1 = \Delta_1(0)/k_B T_c$ and $\alpha_2 = \Delta_2(0)/k_B T_c$ with their respective weights γ_1/γ_m and γ_2/γ_{el} .

To calculate the theoretical curves $c_{el}/\gamma_{el} T$ the parameters Δ_1 , Δ_2 , their respective ratios γ_1 and γ_2 and the ratio γ_{res}/γ_{el} are left for free in fitting (γ_{res} represents the non-negligible residual value at low- T). The best description of the experimental data is obtained using values of $\Delta_1/k_B T_c = 0.46$ and $\Delta_2/k_B T_c = 1.75$. The calculated specific heat data are represented by the solid blue line in Fig. 8 (upper panel). Anyhow, small relative jumps are not compatible with the strong coupling scenario estimated in Fig. 4 for the case of no extrinsic contributions. Therefore we performed a second analysis where the effective extrinsic linear contribution necessary for a weak coupling scenario has been subtracted from the raw data. The result is shown in the lower panel of Fig. 8. Then both gaps do slightly increase: 1.8 K and 6.2 K.

Naturally, the obtained gap values are smaller than the largest gap in e.g. the optimally hole doped $\text{Ba}_{0.6}\text{K}_{0.4}\text{Fe}_2\text{As}_2$ as observed by ARPES investigations [61] but comparable to the two-band s -wave fit for the penetration depth data ($H \parallel c$: 1.28 K and 5.57 K but do not clearly exceed the corresponding values for the isomorphic compound RbFe_2As_2 system with a slightly lower T_c -value of 2.52 K, only: 1.74 K and 5.7 K. [58]. In our opinion this might reflect the presence of nodes in the superconducting order parameter of KFe_2As_2 . Anyhow, a detailed comparison of these two closely related systems would be very interesting, especially, if in fact it would be confirmed that the symmetry of the order parameter would be different.

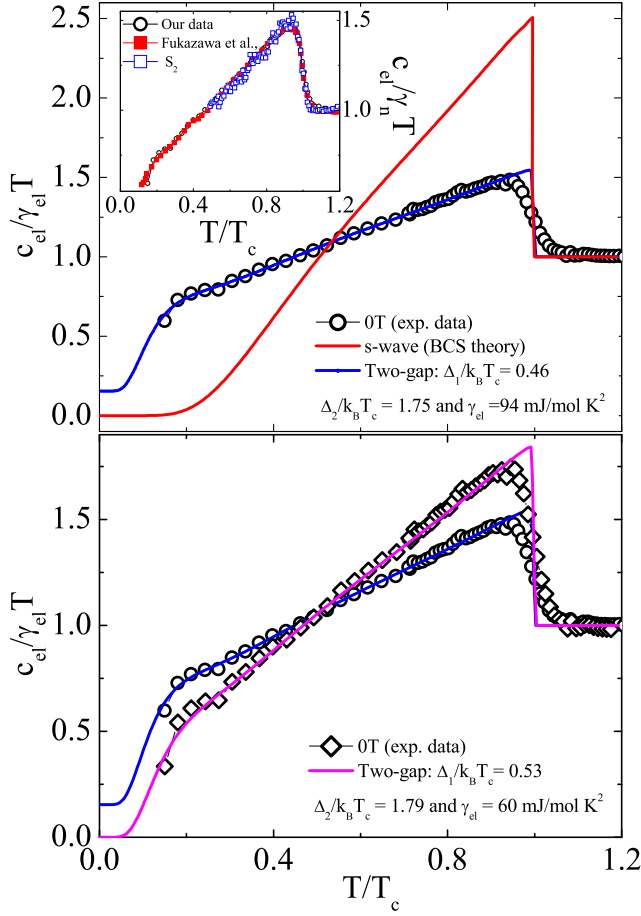


FIG. 8: (Color online) Upper panel: Fit under the assumption of no extrinsic contribution to the linear specific heat (see also Figs. 3 and 4). The normalized superconducting electronic specific heat $c_{el}/(\gamma_{el}T)$ of KFe_2As_2 as a function of the reduced temperature $t = T/T_c$. The red line represents the theoretical curve for the single-band weak coupling BCS case ($\Delta_0/k_B T_c = 1.76$). The blue line shows the curve of the nodeless weakly coupled two-gap model fit; for details see text. The inset shows our electronic specific heat data in comparison with data by Fukazawa *et al.*, [21] together with an another sample which has been shown that our T_c is similar to the investigated sample. Lower panel: fit assuming that a significant contribution to the linear specific heat is not intrinsic: using e.g. $\gamma_{el} = 60 \text{ mJ/mol K}^2$ taken from Ref. 20 (see Figs. 3 and 4.).

Although a clear picture is still missing for the case of KFe_2As_2 , it is important to emphasize that our system definitely underlies multiband superconductivity, probably in the weak coupling regime. However, from specific heat data alone it is difficult to be sure whether nodes exist or not, since in the case of multi-band superconductivity low-energy quasi-particle excitations can be always explained by the contribution from an electron group with a small gap. We believe that further experimental studies such as specific heat well below 400 mK, ARPES and transport investigations at very low T , will be helpful to elucidate the nature of superconductivity in

KFe_2As_2 .

IV. CONCLUSIONS

In summary, KFe_2As_2 was investigated by ac susceptibility and low- T specific heat measurements on high-quality single crystals grown by a self-flux technique. The specific heat jump was found to be $\Delta c_{el}/T_c \sim 45.9 \text{ mJ/mol K}^2$ and the nominal Sommerfeld coefficient $\gamma_n = 94(3) \text{ mJ/mol K}^2$. However, several theoretical considerations including two recently proposed modified Kadowaki-Woods relations as well as the observation of a significant linear in T residual term point to a significantly *smaller* value for the itinerant quasi-particles of about $60 \text{ mJ/K}^2 \text{ mol}$. This way the strongly correlated "heavy-fermion-like" scenario suggested for K-122 in the literature should be revisited. In this context the elucidation of the "external" subsystem responsible for that difference is a challenging problem to be considered elsewhere. The total electron-boson coupling constant $\lambda_{\text{tot}} = \lambda_{\text{ph}} + \lambda_{\text{sf}} \sim 1$ averaged over all Fermi surfaces excludes strong coupling. The calculated weak electron-phonon coupling of about 0.17 points to a dominant spin-fluctuation mechanism and unconventional superconductivity.

The magnetic phase diagram has been studied yielding values for the upper critical fields $\mu_0 H_{c2}^c(0) \approx 1.4 \text{ T}$ and $\mu_0 H_{c2}^{ab}(0) \approx 7 \text{ T}$ for the c axis and ab plane, respectively. The resulting anisotropy of KFe_2As_2 near T_c lies around $\Gamma = H_{c2}^{(ab)}/H_{c2}^{(c)} \sim 5$ which slightly exceeds the mass anisotropy as derived from DFT-electronic structure calculations as well as the anisotropy of the penetration depth. Additionally, the T -dependence of our zero-field electronic specific heat c_{el} cannot be described within single-band weak-coupling BCS theory.

For a full understanding of the gap structure of KFe_2As_2 as well as of the high values of $c_{el}/\gamma_{el}T$ at low temperatures, further specific heat measurements at very low $T < 400 \text{ mK}$ and/or low- T ARPES and transport studies will be helpful. Finally, the irreversibility field H_{irr} derived from ac susceptibility data has been investigated. The double-maximum in $\chi''_v(T)$ for $H||c$ suggests the presence of a peak effect in the T -dependence of the critical current.

Acknowledgments

The authors thank V. Zabolotnyy, A. Chubukov, G. Fuchs and S. Borisenko for fruitful discussions and M. Deutschmann, S. Müller-Litvanyi, R. Müller, J. Werner, S. Pichl, and S. Gass and K. Nenkov for technical support. This project was supported by the DFG through SPP 1458 and Grants No. GR3330/2 and BE1749/13. SW acknowledges support by DFG under the Emmy-Noether program (Grant No. WU595/3-1). Financial

support by the Pakt for Forschung at the IFW-Dresden is also acknowledged by V.G and S.-L.D. S.J. thanks the Foundation for Fundamental Research on Matter (The

Netherlands) for financial support.

-
- [1] Y. Kamihara, T. Watanabe, M. Hirano, and H. Hosono, *J. Am. Chem. Soc.* **130**, 3296 (2008).
- [2] H. Fukazawa, Y. Yamada, K. Kondo, Y. Kohori, K. Kuga, Y. Matsumoto, S. Nakatsuji, H. Kito, P.M. Shirage, K. Kihou *et al.*, *J. Phys. Soc. Jpn.* **78**, 083712 (2009).
- [3] K. Kihou, T. Saito, S. Ishida, M. Nakajima, Y. Tomioka, H. Fukazawa, Y. Kohori, T. Ito, S. Uchida, A. Iyo *et al.* *J. Phys. Soc. Jpn.* **79**, 124713 (2010).
- [4] T. Terashima, M. Kimata, H. Satsukawa, A. Harada, K. Hazama, S. Uji, H. Harima, G.-F. Chen, J.-L. Luo, and N.-L. Wang, *J. Phys. Soc. Jpn.* **78**, 063702 (2009).
- [5] T. Sato, K. Nakayama, Y. Sekiba, P. Richard, Y.-M. Xu, S. Souma, T. Takahashi, G.F. Chen, J.L. Luo, N.L. Wang and H. Ding, *Phys. Rev. Lett.* **103**, 047002 (2009).
- [6] D.V. Evtushinsky, private communication.
- [7] C.H. Lee, K. Kihou, H. Kawano-Furukawa, T. Saito, A. Iyo, H. Eisaki, H. Fukazawa, Y. Kohori, K. Suzuki, H. Usui, K. Kuroki, and K. Yamada, *Phys. Rev. Lett.* **106**, 067003 (2011).
- [8] T. Terashima, M. Kimata, N. Kurita, H. Satsukawa, A. Harada, K. Hazama, M. Imai, A. Sato, K. Kihou, C.-H. Lee, *et al.*, *J. Phys. Soc. Jpn.* **79**, 053702 (2010).
- [9] M. Kimata, T. Terashima, N. Karita, H. Satsukawa, A. Harada, K. Kadoma, K. Takehana, Y. Imanaka, T. Takamasu, K. Kihou *et al.*, *Phys. Rev. Lett.* **107**, 166402 (2011).
- [10] U. Welp, C. Chaparro, A.E. Koshelev, W.K. Kwok, A. Rydh, N.D. Zhigadlo, J. Karpinski, and S. Weyeneth, *Phys. Rev. B* **83**, 100513(R) (2011).
- [11] J.L. Zhang, L. Liao, Y. Chen, and H.Q. Yuan, *Front. Phys.* **2011**, 463 (2012); arXiv:1201.2548 (2012).
- [12] V.G. Kogan, *Phys. Rev. B* **80**, 214532 (2009).
- [13] Kim *et al.* [14] have also studied the magnetic phase diagram of KFe_2As_2 by specific heat measurements. However, in their studies they used a batch of several single crystals glued on top of each other, which is less favorable than using only one piece of single crystalline material.
- [14] J.S. Kim, E.G. Kim, G.R. Stewart, X.H. Chen, and X.F. Wang, *Phys. Rev. B* **83**, 172502 (2011).
- [15] M.I. Tsindlekht, I. Felner, M. Zhang, A.F. Wang, and X.H. Chen, *Phys. Rev. B* **84**, 052503 (2011).
- [16] J. A. Osborn, *Phys. Rev.* **67**, 351 (1945).
- [17] F. Gömöry, *Supercond. Sci. Technol.* **10**, 523 (1997).
- [18] J. Giapintzakis, R.L. Neiman, and D.M. Ginsberg, *Phys. Rev. B* **50**, 16001 (1994).
- [19] E.S. Vlahov, K. Nenkov, M. Ciszek, A. Zaleski, and Y. Dimitriev, *Physica C* **225**, 149 (1994).
- [20] V.A. Grinenko, M. Abdel-Hafez, S. Aswartham, M. Kumar, C. Hess, S. Wurmehl, K. Nenkov, A.U.B. Wolter, S.-L. Drechsler and, B. Büchner, arXiv:1203.1585 (2012).
- [21] H. Fukazawa, T. Saito, Y. Yamada, K. Kondo, M. Hirano, Y. Kohori, K. Kuga, A. Sakai, Y. Matsumoto, S. Nakatsuji *et al.*, *J. Phys. Soc. Jpn.* **80**, SA118 (2011).
- [22] P. Popovich, A.V. Boris, O.V. Dolgov, A.A. Dolgov, D.L. Sun, C.T. Lin, R.K. Kremer, and B. Keimer, *Phys. Rev. Lett.* **105**, 027003 (2010).
- [23] G. Mu, H. Luo, Z. Wang, L. Shan, C. Ren, and H.-H. Wen, *Phys. Rev. B* **79**, 174501 (2009).
- [24] A.K. Pramanik, M. Abdel-Hafez, S. Aswartham, A.U.B. Wolter, S. Wurmehl, V. Kataev, and B. Büchner, *Phys. Rev. B* **84**, 064525 (2011).
- [25] K. Hashimoto, A. Serafin, S. Tonegawa, R. Katsumata, R. Okazaki, T. Saito, H. Fukazawa, Y. Kohori, K. Kihou, C.H. Lee, A. Iyo, H. Eisaki, H. Ikeda, Y. Matsuda, A. Carrington, and T. Shibauchi, *Phys. Rev. B* **82**, 014526 (2010).
- [26] H. Rosner *et al.* in preparation.
- [27] S.-L. Drechsler, H. Rosner *et al.* arXiv:0904.0827 (2009).
- [28] This estimate is based on the slightly higher experimental values of about 1.6 eV observed for less hole-doped samples [22, 27] and the correspondingly slightly larger bare values from DFT-calculations 2.63 to 2.7 eV [27].
- [29] Hussey, *J. Phys. Soc. Jpn.* **74**, 1107 (2005).
- [30] A.C. Jacko, J.O. Hjarestadt, and B.J. Powell, *Nature Phys.* **5**, 422 (2009).
- [31] L. Boeri, O.V. Dolgov, and A.A. Golubov, *Phys. Rev. Lett.* **101**, 026403 (2008); and further work in preparation.
- [32] H. Kawano-Furukawa, C.J. Bowell, J.s. White, R.w. Heslop, A.s. Cameron, E.M. Forgan, K. Kihou, C.H. Lee, A. Yyo, H. Eisaki, T. Saito, H. Fukuzawa *et al.* *Phys. Rev. B* **84**, 024507 (2011).
- [33] S.-L. Drechsler, M. Grobosch, R. Schuster, B. Büchner, and M. Knupfer, *Phys. Rev. Lett.* **101**, 257004 (2008).
- [34] S.-L. Drechsler, F. Roth, M. Grobosch, R. Schuster, K. Koepernik, H. Rosner, G. Behr, M. Rotter, D. Johrendt, B. Büchner, and M. Knupfer, *Physica C* **470**, S332 (2010).
- [35] The trivial case of a corresponding considerable number of electrons not involved in the superconducting condensate can be excluded by Eq. (6) which in such a case yields: $(n_s/n)2.64 = 2.28 = (1 + \lambda_{ph} + \lambda_{sf})(1 + \delta)$. Using even $\lambda_{ph} \sim 0.15$ for the remaining 75% of superconducting electrons, one is left for the same small disorder parameter $\delta = 1/3$ with $\lambda_{sf} \approx 0.3$, only, which is too small to explain the observed T_c -value as discussed elsewhere. Only in the unrealistic absolute clean limit $\delta = 0$ one would be left with $\lambda_{sf} \approx 0.8$ and a reasonable T_c -value of 4 to 5 K. Thereby a broad spectral Eliashberg function for the experimentally observed spin fluctuations centered at about 90.5 K [7] has been used in our strong coupling calculations.
- [36] We stress that the small disorder adopted in the present analysis using Eqs. (5,6) is not applicable to our samples but only to that superclean sample of Ref. 32 for which the small penetration depth has been reported.
- [37] J.A. Woollam, R.B. Somoano, and P.O. Connor, *Phys. Rev. Lett.* **32**, 712 (1974).
- [38] C.K. Jones, J.K. Hulm, and B.S. Chandrasekhar, *Rev. Mod. Phys.* **36**, 74 (1964).
- [39] K. Ohishi, Y. Ishii, H. Fukazawa, T. Saito, I. Watanabe,

- Y. Kohori, T. Suzuki, K. Kihou, C.-H. Lee, K. Miyazawa, H. Kito, A. Iyo, and H. Eisaki, arXiv:1112.6078v1 (2012).
- [40] H. Nakamura, M. Machida, T. Koyama, and N. Hamada, J. Jpn. Phys. Soc. **78**, 123712 (2009).
- [41] N.R. Werthamer, E. Helfand, and P.C. Hohenberg: Phys. Rev. **147**, 295 (1966).
- [42] V. Grinenko, K. Kikoin, S.-L. Drechsler, G. Fuchs, K. Nenkov, S. Wurmehl, F. Hammerath, G. Lang, H.-J. Grafe, B. Holzapfel, J. van den Brink, B. Büchner, and L. Schultz, Phys. Rev. B **84**, 134516 (2011).
- [43] A. Gurevich, Phys. Rev. B **67**, 184515 (2003).
- [44] A. Gurevich, Rep. Progr. Phys. **74**, 124501 (2011).
- [45] C. Tarantini, A. Gurevich, J. Jaroszynski, F. Balakirev, E. Belingeri, I. Pallecchi, C. Ferdeghini, B. Shen, H.H. Wen, and D.C. Larbalestier, Phys. Rev. B **84**, 184522 (2011).
- [46] Starting with the BCS-expression for the Pauli-limiting field for a d -wave superconductor $2.25T_c = 6.3$ T which is somewhat smaller than the WHH-orbital field of 7.37 T and using the experimental data of Terashima *et al.* [4], one concludes that for their sample the paramagnetic pair breaking should in fact play some role. However, this data can be fitted alternatively with a significantly smaller Maki parameter α and with a nearly isotropic spin-orbit coupling constant. (Our full relativistic band structure calculation predict a 10% change both for the mass anisotropy and for the Fermi velocities as compared with usually employed scalar relativistic ones.) Then one extrapolates $\mu_0 H_{c2,ab}^*(0) = 7.0$ T for $\lambda_{sO} = 0.1$, $\alpha = 1.4$, and the Pauli-limited field of $\mu_0 H_{c2,ab} = 4.4$ T. Thereby the fitted slope for the (ab) -direction is slightly reduced to -3.6 T/K which seems to be still within the error bars of the slope of -3.8 T/K reported there. Thus, we arrive at a slope anisotropy near T_c of 5.07 instead of 6.8 as claimed in Ref. 4, but very close to our value of 5.05 reported above. The obtained empirical Pauli limiting field of 6.25 T is very close to the d -wave BCS-estimate given above which points again to a weak coupling scenario. Thus, in our interpretation of the data of Ref. 4 the anisotropy at $T = 0$ is reduced to 3.68 due to the Pauli limiting. We ascribe that Pauli-limiting behavior, absent in our cleaner samples, to an enlarged concentration of magnetic moments involved in the pair-breaking subsystem which enhances the effective Pauli-susceptibility in governing the paramagnetic effect according to the Wolff-mechanism [42].
- [47] Y. Jia, P. Cheng, L. Fang, H. Luo, H. Yang, C. ren, L. Shan, C. Gu, H.-H. Wen, Appl. Phys. Lett. **93**, 032503 (2008).
- [48] J. J. Hamlin, R. E. Baumbach, D. A. Zocco, T. A. Sayles, M. B. Maple, J. Phys. Cond. Mat. **20**, 365220 (2008).
- [49] U. Welp, R. Xie, A.E. Koshelev, W.K. Kwok, H.Q. Luo, Z.S. Wang, G. Mu and H.H. Wen, Phys. Rev. B **79**, 094505 (2009).
- [50] H.Q. Yuan, J. Singleton, F. F. Balakirev, S.A. Baily, G.F. Chen, J.L. Luo, and N. L. Wang, Nature **457**, 565 (2009).
- [51] E. Backen, S. Haindl, T. Niemeier, R. Hühne, J. Freudenberger, J. Werner, G. Behr, L. Schultz, and B. Holzapfel, Supercond. Sci. Technol. **21**, 122001 (2008).
- [52] J. Bardeen, L. N. Cooper, and J. R. Schrieffer, Phys. Rev. **108**, 1175 (1957).
- [53] K. Deguchi, Z.Q. Mao, H. Yaguchi, and Y. Maeno, Phys. Rev. Lett. **92**, 947002 (2004).
- [54] K. Naoyuki *et al.*, J. Phys. Soc. Jpn. **79**, 113702 (2010).
- [55] F. Hardy, T. Wolf, R.A. Fisher, R. Eder, P. Schweiss, P. Adelman, H. Löhneysen, and C. Meingast, Phys. Rev. B **81**, 060501(R) (2010).
- [56] I.I. Mazin, D.J. Singh, M.D. Johannes, and M.H. Du, Phys. Rev. Lett. **101**, 057003 (2008).
- [57] M. Yashima, H. Nishimura, H. Mukada, Y. Kitaoka, K. Miyazawa, P.M. Shirage, K. Kihou, H. Kito, H. Eisaki, and A. Iyo, J. Phys. Soc. Jpn. **78**, 103702 (2009).
- [58] Z. Shermadini, J. Kanter, C. Baines, M. Bendele, Z. Bukowski, R. Khasanov, H.-H. Klauss, H. Luetkens, H. Maeter, G. Pascua, B. Batlogg, and A. Amato, Phys. Rev. B **82**, 144527 (2010).
- [59] F. Bouquet, Y. Wang, R.A. Fisher, D.G. Hinks, J.D. Jorgensen, A. Junod, and N.E. Phillips. Europhys. Lett. **56**, 856 (2001).
- [60] B. Mühlischlegel, Z. Phys. **155**, 313 (1959).
- [61] H. Ding, P. Richard, K. Nakayama, K. Sugawara, T. Arakane, Y. Sekiba, A. Takayama, S. Souma, T. Sato, T. Takahashi Z. Wang, X. Dai, Z. Fang, G.F. Chen, J.L. Luo and N.L. Wang, Europhys. Lett. **83**, 47001 (2008).